

1  
2  
3  
4  
5  
6  
7  
8  
9  
10  
11  
12  
13  
14  
15  
16  
17  
18  
19  
20  
21  
22

**On the observational determination of climate sensitivity and its implications**

Richard S. Lindzen<sup>\*</sup>, and Yong-Sang Choi<sup>†</sup>

<sup>\*</sup>Program in Atmospheres, Oceans, and Climate, Massachusetts Institute of Technology,  
Cambridge, MA 02142 USA

<sup>†</sup>Department of Environmental Science and Engineering, Ewha Womans University,  
Seoul, 120-750 Korea

October 19, 2010

Proceedings of the National Academy of Sciences of the United States of America

(revised)

Corresponding author: Prof. Richard S. Lindzen, E-mail: rlindzen@mit.edu.

23 **Abstract**

24 We estimate climate sensitivity from observations, using the deseasonalized fluctuations in sea  
25 surface temperatures (SSTs) and the concurrent fluctuations in the top-of-atmosphere (TOA)  
26 outgoing radiation from the ERBE (1985-1999) and CERES (2000-2008) satellite instruments.  
27 Distinct periods of warming and cooling in the SSTs were used to evaluate feedbacks. An earlier  
28 study (Lindzen RS, Choi Y-S (2009) *Geophys Res Lett* 36:L16705) was subject to significant  
29 criticisms. The present paper is an expansion of the earlier paper where the various criticisms are  
30 taken into account. The present analysis accounts for the 72 day precession period for the ERBE  
31 satellite in a more appropriate manner than in the earlier paper. We also attempt to distinguish  
32 noise in the outgoing radiation as well as radiation changes that are forcing SST changes from  
33 those radiation changes that constitute feedbacks to changes in SST. We argue that feedbacks are  
34 largely concentrated in the tropics; however, the tropical feedbacks are adjusted to account for  
35 their impact on the globe as a whole. We again find that the outgoing radiation resulting from  
36 SST fluctuations exceeds the zero-feedback response thus implying negative feedback. In  
37 contrast to this, the calculated TOA outgoing radiation fluxes from 11 atmospheric models  
38 forced by the observed SST are less than the zero-feedback response, consistent with the positive  
39 feedbacks that characterize these models. The results imply that the models are exaggerating  
40 climate sensitivity.

41 **\body**

42

43 **1. Introduction**

44 The heart of the global warming issue is so-called greenhouse warming. This refers to the fact  
45 that the earth balances the heat received from the sun (mostly in the visible spectrum) by  
46 radiating in the infrared portion of the spectrum back to space. Gases that are relatively  
47 transparent to visible light but strongly absorbent in the infrared (greenhouse gases) interfere  
48 with the cooling of the planet, forcing it to become warmer in order to emit sufficient infrared  
49 radiation to balance the net incoming sunlight. By net incoming sunlight, we mean that portion  
50 of the sun's radiation that is not reflected back to space by clouds, aerosols and the earth's  
51 surface. CO<sub>2</sub>, a relatively minor greenhouse gas, has increased significantly since the beginning  
52 of the industrial age from about 280 ppmv to about 390 ppmv, presumably due mostly to man's  
53 emissions. This is the focus of current concerns. However, warming from a doubling of CO<sub>2</sub>  
54 would only be about 1°C (based on simple calculations where the radiation altitude and the  
55 Planck temperature depend on wavelength in accordance with the attenuation coefficients of  
56 well-mixed CO<sub>2</sub> molecules; a doubling of any concentration in ppmv produces the same  
57 warming because of the logarithmic dependence of CO<sub>2</sub>'s absorption on the amount of CO<sub>2</sub>) (1).

58 This modest warming is much less than current climate models suggest for a doubling of  
59 CO<sub>2</sub>. Models predict warming of from 1.5°C to 5°C and even more for a doubling of CO<sub>2</sub>.  
60 Model predictions depend on the 'feedback' within models from the more important greenhouse  
61 substances, water vapor and clouds. Within all current climate models, water vapor increases  
62 with increasing temperature so as to further inhibit infrared cooling. Clouds also change so that  
63 their visible reflectivity decreases, causing increased solar absorption and warming of the earth.

64 Cloud feedbacks are still considered to be highly uncertain (1), but the fact that these  
65 feedbacks are strongly positive in most models is considered to be an indication that the result is

66 basically correct. Methodologically, this is unsatisfactory. Ideally, one would seek an  
67 observational test of the issue. Here we suggest that it may be possible to test the issue with  
68 existing data from satellites.

69 Indeed, an earlier study by Forster and Gregory (2) examined the anomaly of the annual  
70 mean temperature and radiative flux observed from a satellite. However, with the annual time  
71 scale, the signal of short-term feedback associated with water vapor and clouds can be  
72 contaminated by unknown time-varying radiative forcing in nature, and the accurate feedbacks  
73 cannot be diagnosed (3). In a recent paper (4) we attempted to resolve these issues though, as we  
74 will show in this paper, the details of that paper were, in important ways, also incorrect (5-7).  
75 There were four major criticisms to Lindzen and Choi (4): (i) statistical insignificance of the  
76 results, (ii) misinterpretation of air-sea interaction in the Tropics, (iii) misuse of uncoupled  
77 atmospheric models, and (iv) incorrect computation of climate sensitivity. The present paper  
78 responds to the criticism, and corrects the earlier approach. The earlier results are not  
79 significantly altered.

80

## 81 **2. Feedback formalism**

82 In the absence of feedbacks, the behavior of the climate system can be described by Fig. 1a  
83  $\Delta Q$  is the radiative forcing,  $G_0$  is the zero-feedback response function of the climate system, and  
84  $\Delta T_0$  is the response of the climate system in the absence of feedbacks. The checkered circle is a  
85 node. Fig. 1a symbolically shows the temperature increment,  $\Delta T_0$ , that a forcing increment,  $\Delta Q$ ,  
86 would produce with no feedback,

$$87 \quad \Delta T_0 = G_0 \Delta Q \quad (1)$$

88 It is generally accepted that in the absence of feedback, a doubling of CO<sub>2</sub> will cause a forcing of

89  $\Delta Q \approx 3.7 \text{ Wm}^{-2}$  and will increase the temperature by  $\Delta T_0 \approx 1.1 \text{ K}$  (8, 9). We therefore take the  
 90 zero-feedback response function of Eq. (1) to be  $G_0 \approx 0.3 (=1.1/3.7) \text{ K W}^{-1} \text{ m}^2$  for the earth as a  
 91 whole.

92 With feedback, Fig. 1a is modified to Fig. 1b. The response is now

$$93 \quad \Delta T = G_0(\Delta Q + F \Delta T) \quad (2)$$

94 Here  $F$  is a feedback function that represents all changes in the climate system (for example,  
 95 changes in cloud cover and humidity) that act to increase or decrease feedback-free effects. Thus,  
 96  $F$  should not include the zero-feedback (ZFB) response to  $\Delta T$  that is already incorporated into  
 97  $G_0$ . The choice of ZFB response for the tropics in Lindzen and Choi (4) is certainly incorrect in  
 98 this respect (5, 6). At present, the best choice seems to remain  $1/G_0$  ( $3.3 \text{ W m}^{-2} \text{ K}^{-1}$ ) (9, 10).

99 Solving Eq. (2) for the temperature increment  $\Delta T$  and inserting Eq. (1) into Eq. (2) we find

$$100 \quad \Delta T = \frac{\Delta T_0}{1 - f} \quad (3)$$

101 The dimensionless feedback fraction is  $f = F G_0$ . Also, dividing Eq. (2) by  $G_0$ , we obtain

$$102 \quad -\frac{f}{G_0} \Delta T = \Delta Q - \frac{\Delta T}{G_0} \quad (4)$$

103 When looking at the observations,  $\Delta Q$  and  $\Delta T$  in Eq. (4) may be replaced by the change in  
 104 outgoing net radiative flux,  $\Delta \text{Flux}$ , and the change in sea surface temperature,  $\Delta \text{SST}$ , respectively,  
 105 leading to

$$106 \quad -\frac{f}{G_0} \Delta \text{SST} = \Delta \text{Flux} - \text{ZFB} \quad (5)$$

107 where ZFB indicates the zero-feedback response to  $\Delta \text{SST}$ , i.e.,  $\Delta \text{SST}/G_0$ . The quantities on the  
 108 right side of the equation indicate the amount by which feedbacks supplement ZFB response to

109  $\Delta\text{Flux}$ . At this point, it is crucial to recognize that our equations are predicated on the assumption  
 110 that the  $\Delta\text{SST}$  to which the feedbacks are responding is produced by  $\Delta\text{Flux}$ . Physically, however,  
 111 we expect that any fluctuation in temperature should elicit the same flux regardless of the origin  
 112 of temperature change. Note that the natural forcing,  $\Delta\text{SST}$ , that can be observed, is actually not  
 113 the same as the equilibrium response temperature  $\Delta T$  in Eq. (4). The latter cannot be observed  
 114 since, for the short intervals considered, the system cannot be in equilibrium, and over the longer  
 115 periods needed for equilibration of the whole climate system,  $\Delta\text{Flux}$  at the top of the atmosphere  
 116 (TOA) is restored to zero. The choice of the short intervals may serve to remove some natural  
 117 time-varying radiative forcing that contaminates the feedback signal (3). As explained in  
 118 Lindzen and Choi (4), it is essential, that the time intervals considered, be short compared to the  
 119 time it takes for the system to equilibrate, while long compared to the time scale on which the  
 120 feedback processes operate (which, in the tropics, are essentially the time scales associated with  
 121 cumulonimbus convection). The latter is on the order of days, while the former depends on the  
 122 climate sensitivity, and ranges from years for sensitivities of  $0.5^\circ\text{C}$  for a doubling of  $\text{CO}_2$  to  
 123 many decades for higher sensitivities (11).

124 Recent studies argued that quantification of feedback based on Eq. (5) is inadequate with our  
 125 available tropical domain due to the exchange of energy between the tropics and the extratropics  
 126 (5, 7). However, there are good reasons to consider the tropics; for example, concentration of  
 127 water vapor in the tropics (see supporting information (SI) for more explanation). However,  
 128 when restricting ourselves to tropical feedbacks, Eq. (5) must be replaced by

$$129 \quad 2f \approx -G_0 \left( \frac{\Delta\text{Flux} - \text{ZFB}}{\Delta\text{SST}} \right)_{\text{tropics}} \quad (6)$$

130 where the factor 2 results from the sharing of the tropical feedbacks over the globe following the

131 methodology of Lindzen, Chou and Hou (12), (hereafter LCH01) and Lindzen, Hou and Farrell  
132 (13); that is to say that the contribution of the tropical feedback to the global feedback is only  
133 about half of the tropical feedback. The precise choice of this factor does not affect the major  
134 conclusion of this study (SI for more details).

135 From Eq. (6), the longwave (LW) and shortwave (SW) contributions to  $f$  are given by

$$136 \quad f_{LW} = -\frac{G_0}{2} \left( \frac{\Delta\text{OLR} - \text{ZFB}}{\Delta\text{SST}} \right)_{tropicals} \quad (7a)$$

$$137 \quad f_{SW} = -\frac{G_0}{2} \left( \frac{\Delta\text{SWR}}{\Delta\text{SST}} \right)_{tropicals} \quad (7b)$$

138 Here we can identify  $\Delta\text{Flux}$  as the change in outgoing longwave radiation (OLR) and shortwave  
139 radiation (SWR) measured by satellites associated with the measured  $\Delta\text{SST}$ . Since we know the  
140 value of  $G_0$ , the experimentally determined slope (the quantity on the right side of Eq. (7)) allows  
141 us to evaluate the magnitude and sign of the feedback factor  $f$  provided that we also know the  
142 value of the ZFB response ( $\Delta\text{SST}/G_0$  in this study). For observed variations, the changes in  
143 radiation (associated for example with volcanoes or non-feedback changes in clouds) can cause  
144 changes in SST as well as respond to changes in SST, and there is a need to distinguish these two  
145 possibilities. This is less of an issue with model results from AMIP (Atmospheric Model  
146 Intercomparison Project) where observed variations in SST are specified. Of course, there is  
147 always the problem of noise arising from the fact that clouds depend on factors other than  
148 surface temperature, and this is true for AMIP as well as for nature. Note that this study deals  
149 with observed outgoing fluxes, but does not specifically identify the origin of the changes (see SI  
150 for more details).

151

### 152 **3. The data and their problems**

153 SST is measured (14), and is always fluctuating (viz. Fig. 2). To relate this SST with the flux  
154 in the entire tropics, the SST anomaly was scaled by a factor of 0.78 (the area fraction of the  
155 ocean to the tropics). High frequency fluctuations, however, make it difficult to objectively  
156 identify the beginning and end of warming and cooling intervals (5). This ambiguity is  
157 eliminated with a 3 point centered smoother. (A two point lagged smoother works too.) In  
158 addition, the net outgoing radiative flux from the earth has been monitored since 1985 by the  
159 ERBE (Earth Radiation Budget Experiment) instrument (15) (nonscanner edition 3) aboard  
160 ERBS (Earth Radiation Budget Satellite) satellite, and since 2000 by the CERES (Clouds and the  
161 Earth's Radiant Energy System) instrument (ES4 FM1 edition 2) aboard the Terra satellite (16).  
162 The results for both LW radiation and SW radiation are shown in Fig. 3. The sum is the net  
163 outgoing flux.

164 With ERBE data, there is the problem of satellite precession with a period of 72 days,  
165 although in the deep tropics all clock hours are covered in 36 days. In Lindzen and Choi (4) that  
166 used ERBE data, we attempted to avoid this problem (which is primarily of concern for the short  
167 wave radiation) by smoothing data over 7 months. It has been suggested (7) that this is excessive  
168 smoothing. In the present paper, we start by taking 36 day means rather than monthly means.  
169 The CERES instrument is flown on a sun-synchronous satellite for which there is no problem  
170 with precession. Thus for the CERES instrument we use the conventional months. However, here  
171 too, we take a 3 point smoothing in the flux data to minimize the effect of noise. This is also why  
172 we use the 36-day averaged SST for 1985–1999 and monthly SST for 2000–2009 in Fig. 2.

173 The discontinuity between the two datasets requires comment. There is the long-term  
174 discrepancy of the average which is believed to be due to the absolute calibration problem (up to  
175  $3 \text{ W m}^{-2}$ ) (17). With CERES, we attempt to resolve the spectral darkening problem by



176 multiplying SW flux by the scale factor (up to 1.011) from Matthews et al. (18). However, this  
177 long-term stability should not matter for our analysis which considers fluctuations over a few  
178 months for which the drift is insignificant. There is also the higher seasonal fluctuation in  
179 CERES SW radiation than in ERBE. The bias is up to  $6.0 \text{ W m}^{-2}$  as estimated by Young et al.  
180 (19). This is attributed to different sampling patterns; ie, ERBS observes all local times over a  
181 period of 72 days, while Terra observes the region only twice per day (around 10:30 AM and  
182 10:30 PM). To avoid this problem, we reference the anomalies for radiative flux separately to the  
183 monthly means for the period of 1985 through 1989 for ERBE, and for the period of 2000  
184 through 2004 for CERES. However, the issue of the reference period is also insignificant in this  
185 study that uses enough segments to cancel out this seasonality.

186 The quality of ERBE and CERES data are best in the tropics. The ERBE field-of-view is  
187 between  $60^{\circ}\text{S}$  and  $60^{\circ}\text{N}$ . For latitudes  $40^{\circ}$  to  $60^{\circ}$ , 72 days are required instead of 36 days to  
188 reduce the precession effect (17). Both datasets have no/negligible shortwave radiation in winter  
189 hemispheric high latitudes, which would compromise our analysis. Moreover, our analysis  
190 involves relating changes in outgoing flux to changes in SST. This is appropriate to regions that  
191 are mostly ocean covered like the tropics or the southern hemisphere, but distinctly inappropriate  
192 to the northern extratropics. However, we believe that the water vapor feedback is primarily  
193 restricted to the tropics, and there are reasons to suppose that this is also the case for cloud  
194 feedbacks (SI). The methodology developed in LCH01 permits the easy evaluation of the  
195 contribution of tropical processes to global values. As noted by LCH01, this does not preclude  
196 there being extratropical contributions as well, but these are not considered in the present paper.

197 Finally, there is the serious issue of distinguishing atmospheric phenomena involving changes  
198 in outgoing radiation that result from processes other than feedbacks (Pinatubo and non-feedback

199 cloud variations for example) and which cause changes in SST, from those that are caused by  
200 changes in SST (namely the feedbacks we wish to evaluate) (5, 6). Our crude approach to this is  
201 to examine the effect of fluxes with time lags and leads relative to temperature changes. The lags  
202 and leads examined are from one to five months. Our procedure will be to choose lags that  
203 maximize R (the correlation). This is discussed in Materials and Methods. To be sure, Fourier  
204 transform methods wherein one investigates phase leads and lags might normally be cleaner, but,  
205 given the gaps in the radiation data as well as the incompatibilities between ERBE and CERES,  
206 the present approach which focuses on individual warming and cooling events seems more  
207 appropriate.

208 Turning to the models, AMIP is responsible for intercomparing atmospheric models used by  
209 the IPCC (the Intergovernmental Panel on Climate Change); the AMIP models are forced by the  
210 same observed SSTs shown in Fig. 2. We have obtained the calculated changes in both SW and  
211 LW radiation from the AMIP models. These results are shown in Figs. S4 and S5 where the  
212 observed results are also superimposed for comparison. We can already see that there are  
213 significant differences. In addition, we will also consider results from CMIP (the Coupled Model  
214 Intercomparison Project), where coupled ocean-atmosphere models were intercompared.

215

## 216 **4. Results**

### 217 **4.1. Climate sensitivity in observation and comparison to AMIP models**

218 Given the above, it is now be possible to directly test the ability of models to adequately  
219 simulate the sensitivity of climate (see Materials and Methods). Fig. 4 shows the impact of  
220 smoothing and leads and lags on the determination of the slope as well as on the correlation, R,  
221 of the linear regression. For LW radiation, the situation is fairly simple. Smoothing increases R

222 somewhat, and for 3 point symmetric smoothing, R maximizes for slight lag or zero – consistent  
223 with the fact that feedbacks are expected to result from fast processes. Maximum slope is found  
224 for a lag of 1 ‘month’, though it should be remembered that the relevant feedback processes may  
225 operate on a time scale shorter than we resolve. The situation for SW radiation is, not  
226 surprisingly, more complex since phenomena like the Pinatubo eruption and non-feedback cloud  
227 fluctuations lead to changes in SW reflection and associated fluctuations in surface temperature.

228 We see two extrema associated with changing lead/lag. There is a maximum negative slope  
229 associated with a brief lead, and a relatively large positive slope associated with a 3–4 month lag.  
230 It seems reasonable to suppose that the effect of anomalous forcing extends into the results at  
231 small lags because it takes time for the ocean surface to respond, and is only overcome for larger  
232 lags where the change in flux associated with feedback dominates. Indeed, excluding the case of  
233 Pinatubo volcano for larger lags does little to change the results (less than  $0.3 \text{ W m}^{-2} \text{ K}^{-1}$ ). Under  
234 such circumstances, we expect the maximum slope for SW radiation in Fig. 4 to be an  
235 underestimate of the actual feedback. We also consider the standard error of the slope to show  
236 data uncertainty.

237 The results for the lags associated with maximum R are shown in Table 1. We take LW and  
238 SW radiation for lag = 1 and lag = 3, respectively, and measure the slope  $\Delta\text{Flux}/\Delta\text{SST}$  for the  
239 sum of these fluxes. The standard error of the slope in total radiation for the appropriate lags  
240 comes from the regression for scatter plots of  $(\Delta\text{SST}, \Delta(\text{OLR}+\text{SWR}))$ . With the slope and its  
241 standard error, the feedback fractions for LW, SW, and total radiation ( $f_{\text{SW}}$ ,  $f_{\text{LW}}$ , and  $f_{\text{Total}}$ ) are  
242 obtained via Eqs. (6) and (7). Finally, with  $f_{\text{Total}}$ , the equilibrium climate sensitivity for a  
243 doubling of  $\text{CO}_2$  is obtained via Eq. (3). Here the statistical confidence intervals of the sensitivity  
244 estimate at 90%, 95%, and 99% levels are also calculated by the standard error of the feedback

245 fraction  $f_{\text{Total}}$ . This interval would prevent any problems arising from limited sampling. As a  
246 result, the climate sensitivity for a doubling of  $\text{CO}_2$  is estimated to be 0.7K (with the confidence  
247 interval 0.5K–1.3K at 99% levels). This observational result shows that model sensitivities  
248 indicated by the IPCC AR4 are likely greater than the possibilities estimated in the observations.

249 We next wish to see whether the outgoing fluxes from the AMIP models are consistent with  
250 the sensitivities in IPCC AR4. To the AMIP results, for which there was less ambiguity as to  
251 whether fluxes constituted a response (noise still exists due to autonomous cloud fluctuations),  
252 the same approach as that for the observations was applied. Maximum R occurs at zero lag in  
253 both LW and SW radiation, so we simply chose the AMIP fluxes without lag. The results are  
254 shown in Table 2. In contrast to the observed fluxes, the implied feedbacks in the models are all  
255 positive, and in one case, marginally unstable. Given the uncertainties, however, one should not  
256 take that too seriously.

257 Table 3 compares the climate sensitivities in K for a doubling of  $\text{CO}_2$  implied by feedback  
258 factors  $f$  in Table 2 with those in IPCC AR4. To indicate statistical significance of our results  
259 obtained from limited sampling, we also calculated the confidence intervals of the climate  
260 sensitivity using the standard errors of  $f$  in Table 2. All the sensitivities in IPCC AR4 are within  
261 the 90% confidence intervals of our sensitivity estimates. The agreement does not seem notable,  
262 but this is because, for positive feedbacks, sensitivity is strongly affected by small changes in  $f$   
263 that are associated standard errors in Table 2. Consequently, the confidence intervals include  
264 “infinity”. This is seen in Fig. 5 in the pink region. It has, in fact, been suggested by Roe and  
265 Baker (20), that this sensitivity of the climate sensitivity to uncertainty in the feedback factor is  
266 why there has been no change in the range of climate sensitivities indicated by GCMs since the  
267 1979 Charney Report (21). By contrast, in the green region, which corresponds to the observed

268 feedback factors, sensitivity is much better constrained.

269

## 270 **4.2. Comparison to CMIP models and their limitations**

271 It has been argued that CMIP models are more appropriate for the present purpose since the  
272 uncoupled AMIP modes are prescribed with incomplete forcings of SST (5). However, it is  
273 precisely for this reason that AMIP models are preferred for our purpose. Note that we are  
274 considering atmospheric feedbacks to SST fluctuations. As already seen, in analyzing observed  
275 behavior, the presence of SST variations that are primarily caused by atmospheric changes (from  
276 volcanoes, non-feedback cloud variations, etc.) leads to difficulty in distinguishing SST  
277 variations that are primarily forcing atmospheric changes (i.e., feedbacks). This situation is much  
278 simpler with AMIP results since we can be sure that SST variations (which are forced to be the  
279 same as observed SST) cannot respond to atmospheric changes. The fact that CMIP SST  
280 variations are significantly different from observed SST variations further makes it unlikely that  
281 the model atmospheric processes are implicitly forcing the SST's used for AMIP. Note that  
282 important ocean phenomena such as El Niño-Southern Oscillation and Pacific Decadal  
283 Oscillation are generally misrepresented by CMIP models. As noted, AMIP results are still  
284 subject to noise since outgoing radiation includes changes associated with non-feedback cloud  
285 variations.

286 In applying our methodology to CMIP, we see that coupled models differ in the behaviors of  
287 SST, and the intervals of SST must be selected differently. Some models have much smaller  
288 variability of SST than nature and only a few intervals of SST could be selected. As we see in  
289 Fig. 6 at a glance, the CMIP results (black dots) display behavior somewhat similar to ERBE and  
290 CERES results (red open circles) with respect to lags. However, when identifying each number,

291 we found that the results are quantitatively ambiguous. The slope  $\Delta\text{OLR}/\Delta\text{SST}$  for lag = 1 is  
292 between 0.6 and 5.8 though it remains robust that LW feedbacks in most models are higher than  
293 nature. Not surprisingly, the inconsistent LW feedback was also shown in previous studies by  
294 Forster and Gregory (2) and Forster and Taylor (22). The slope  $\Delta\text{SWR}/\Delta\text{SST}$  for lag = 3 is  
295 between -3.4 and 3.9 so that one cannot precisely determine the feedback in the models. These  
296 values, moreover, do not correspond well to the independently known model climate sensitivities  
297 in IPCC AR4. Based on our simple model (Materials and Methods), this ambiguity results  
298 mainly from non-feedback internal radiative (cloud-induced) change that changes SST (see Fig.  
299 S3 and SI for more information). Also, such cloud-induced radiative change can generate the  
300 anomalous sinusoidal shape of the slopes  $\Delta\text{SWR}/\Delta\text{SST}$  with respect to lags as shown in Fig. 6.  
301 Therefore, previous studies that use the slopes  $\Delta\text{SWR}/\Delta\text{SST}$  at zero lag (2, 5) may misinterpret  
302 SW feedback. This confirms that for more accurate estimation of ‘model’ feedbacks, AMIP  
303 models are more appropriate than CMIP models. Furthermore, nature is better than CMIP  
304 because nature properly displays the real magnitude of SST forcing and the associated  
305 atmospheric changes, even though it also includes SST response to radiative forcing.

306

## 307 **5. Conclusions and discussions**

308 We have corrected the approach of Lindzen and Choi (4), based on all the criticisms made of  
309 the earlier work (5-7). First of all, to improve the statistical significance of the results, we  
310 supplemented ERBE data with CERES data, filtered out data noise with 3-month smoothing,  
311 objectively chose the intervals based on the smoothed data, and provided confidence intervals for  
312 all sensitivity estimates. These constraints helped us to more accurately obtain climate feedback  
313 factors than with the original use of monthly data. Next, our new formulas for climate feedback

314 and sensitivity reflected sharing of tropical feedback with the globe, so that the tropical region  
315 was identified as an open system. Last, the feedback factors inferred from the atmospheric  
316 models are more consistent with IPCC-defined climate sensitivity than those from the coupled  
317 models. This is because, in the presence of cloud-induced radiative changes altering SST, the  
318 climate feedback estimates by the present approach tends to be inaccurate. With all corrections,  
319 the conclusion appears to be that all current models seem to exaggerate climate sensitivity (some  
320 greatly).

321 Our analysis of the data only demands relative instrumental stability over short periods, and is  
322 largely independent of long term drift. Concerning the different sampling from the ERBE and  
323 CERES instruments, Murphy et al. (23) repeated the Forster and Gregory (2) analysis for the  
324 CERES and found very different values than those from the ERBE. However, in this study, the  
325 addition of CERES data to the ERBE data does little to change the results for  $\Delta\text{Flux}/\Delta\text{SST}$  –  
326 except that its value is raised a little (as is also true when only CERES data is used.).

327 Our study also suggests that, in current coupled atmosphere-ocean models, the atmosphere and  
328 ocean are too weakly coupled since thermal coupling is inversely proportional to sensitivity (11).  
329 It has been noted by Newman et al. (24) that coupling is crucial to the simulation of phenomena  
330 like El Niño. Thus, corrections of the sensitivity of current climate models might well improve  
331 the behavior of coupled models. It should be noted that there have been independent tests that  
332 also suggest sensitivities less than predicted by current models. These tests are based on response  
333 to sequences of volcanic eruptions (11), on the vertical structure of observed versus modeled  
334 temperature increase (25, 26), on ocean heating (9, 27), and on satellite observations (3). Most  
335 claims of greater sensitivity are based on the models that we have just shown can be highly  
336 misleading on this matter. There have also been attempts to infer sensitivity from paleoclimate

337 data (28), but these are not really tests since the forcing is essentially unknown given major  
338 uncertainties in clouds and dust loading.

339 One final point needs to be made. Low sensitivity of global mean temperature anomaly to  
340 global scale forcing does not imply that major climate change cannot occur. The earth has, of  
341 course, experienced major cool periods such as those associated with ice ages and warm periods  
342 such as the Eocene (29). As noted, however, in Lindzen (30), these episodes were primarily  
343 associated with changes in the equator-to-pole temperature difference and spatially  
344 heterogeneous forcing. Changes in global mean temperature were simply the residue of such  
345 changes and not the cause.

## 346 **Materials and Methods**

### 347 **a. Simple model analysis**

348 Following Spencer and Braswell (3), we assume an hypothetical climate system with uniform  
349 temperature and heat capacity, for which SST and forcing are time-varying. Then the model  
350 equation of the system is

$$351 \quad C_p \left[ \frac{d\Delta T}{dt} \right] = Q(t) - F \cdot \Delta T(t) \quad (8)$$

352 where  $C_p$  is the bulk heat capacity of the system ( $14 \text{ yr W m}^{-2} \text{ K}^{-1}$  in this study, from ref. 9);  $\Delta T$   
353 is SST deviation away from an equilibrium state of energy balance;  $F$  is the feedback function  
354 that is the same as the definition in Eq. (2);  $Q$  is any forcing that changes SST (2, 3).  $Q$  is  
355 composed of three sources of forcing: (i) external radiative forcing (from anthropogenic  
356 greenhouse gas emission, e.g.), (ii) internal non-radiative forcing (from heat transfer from ocean,  
357 e.g.), and (iii) internal radiative forcing (from water vapor or clouds, e.g.). Among the three  
358 forcings, the two external and internal ‘radiative’ forcings, and  $F \cdot \Delta T(t)$  constitute TOA net  
359 radiative flux anomaly, i.e.,  $\Delta \text{Flux}$ . This simple model is used, in order to investigate sensitivity



360 of our approach to feedback function and to radiative forcing. Results are shown in SI.

361

### 362 **b. Feedback estimation method**

363 As already noted, the data need to be smoothed first to minimize noise. Then the procedure is  
364 simply to identify intervals of maximum change in  $\Delta\text{SST}$  (red and blue in Fig. 2), and for each  
365 such interval, to find the change in flux. The reasoning for this is that, by definition, a  
366 temperature change is required to produce radiative feedback, and so the greatest signal (and  
367 least noise) in the estimation of feedback should be associated with the largest temperature  
368 changes. Thus, it is advisable, but not essential, to restrict oneself to changes greater than  $0.1^\circ\text{C}$ ;  
369 in fact, the impact of thresholds for  $\Delta\text{SST}$  on the statistics of the results is minor (1). Let us  
370 define  $t_1, t_2, \dots, t_m$  as selected time steps that correspond to the starting and the ending points of  
371 intervals. Again, for stable estimation of  $\Delta\text{Flux}/\Delta\text{SST}$ , the time steps should be selected based on  
372 the maximum and minimum of the smoothed SST.  $\Delta\text{Flux}/\Delta\text{SST}$  can be basically obtained by  
373  $\text{Flux}(t_{i+1}) - \text{Flux}(t_i)$  divided by  $\text{SST}(t_{i+1}) - \text{SST}(t_i)$  where  $t_i$  is  $i$ th selected time steps ( $i = 1, 2, \dots,$   
374  $m-1$ ). As there are many intervals, the final  $\Delta\text{Flux}/\Delta\text{SST}$  is a regression slope for the plots  
375 ( $\Delta\text{Flux}, \Delta\text{SST}$ ) for a linear regression model. Here we use a zero y-intercept model ( $y = ax$ )  
376 because the presence of the y-intercept is related to noise other than feedbacks. Thus, a zero y-  
377 intercept model may be more appropriate for the purpose of our feedback analysis though the  
378 choice of regression model turns out to also be minor.

379 One must also distinguish  $\Delta\text{SST}$ 's that are forcing changes in  $\Delta\text{Flux}$ , from responses to  $\Delta\text{Flux}$ .  
380 Otherwise,  $\Delta\text{Flux}/\Delta\text{SST}$  can vary (5) and/or may not represent feedbacks that we wish to  
381 determine. To avoid such a problem, we use lag-lead methods (e.g., use of  $\text{Flux}(t+\text{lag})$  and  
382  $\text{SST}(t)$ ) for ERBE 36-day and CERES monthly data). In general, the use of leads for flux will

383 emphasize forcing by the fluxes, and the use of lags will emphasize responses by the fluxes to  
384 changes in SST.

385 The above procedures help to obtain a more accurate climate feedback factor than the use of  
386 original monthly data. This was tested by a Monte-Carlo test of the above simple feedback-  
387 forcing model. With minimal cloud-induced radiative changes, our method always gives the  
388 feedback factor close to the true value (Fig. S2), whereas the conventional regression method  
389 with monthly data tends to underestimate the feedback particularly in the presence of increasing  
390 external radiative forcing (e.g., increasing CO<sub>2</sub> forcing) (3).

391

### 392 **Acknowledgements**

393 This research was supported by DOE grant DE-FG02-01ER63257 and by and Korea Science and  
394 Engineering Foundation (KOSEF) Grant by the Korean government (2010-0001904). The  
395 authors thank NASA Langley Research Center and the PCMDI team for the data, and Jens  
396 Vogelgesang, Hyonho Chun, William Happer, Lubos Motl, Tak-meng Wong, Roy Spencer, and  
397 Richard Garwin for helpful suggestions. We also wish to thank Dr. Daniel Kirk-Davidoff for a  
398 helpful question.

399

400 **References**

- 401 1. Intergovernmental Panel on Climate Change (2007) Climate Change 2007: The Physical  
402 Science Basis. Contribution of Working Group I to the Fourth Assessment Report of the  
403 Intergovernmental Panel on Climate Change. Cambridge Univ. Press, Cambridge, U. K.
- 404 2. Forster PM, Gregory JM (2006) The climate sensitivity and its components diagnosed from  
405 Earth Radiation Budget data. *J Climate* 19:39–52.
- 406 3. Spencer RW, Braswell WD (2010) On the diagnosis of radiative feedback in the presence of  
407 unknown radiative forcing. *J Geophys Res* 115:D16109.
- 408 4. Lindzen RS, Choi Y-S (2009) On the determination of climate feedbacks from ERBE data.  
409 *Geophys Res Lett* 36:L16705.
- 410 5. Trenberth KE, Fasullo JT, O’Dell C, Wong T (2010) Relationships between tropical sea  
411 surface temperature and top-of-atmosphere radiation. *Geophys Res Lett* 37:L03702.
- 412 6. Chung E-S, Soden BJ, Sohn BJ (2010) Revisiting the determination of climate sensitivity from  
413 relationships between surface temperature and radiative fluxes. *Geophys Res Lett* 37:L10703.
- 414 7. Murphy DM (2010) Constraining climate sensitivity with linear fits to outgoing radiation.  
415 *Geophys Res Lett* 37:L09704.
- 416 8. Hartmann DL (1994) Global physical climatology. Academic Press, 411 pp.
- 417 9. Schwartz SE (2007) Heat capacity, time constant, and sensitivity of Earth’s climate system. *J*  
418 *Geophys Res* 112:D24S05.
- 419 10. Colman R (2003) A comparison of climate feedbacks in general circulation models. *Climate*  
420 *Dyn* 20:865–873.
- 421 11. Lindzen RS, Giannitsis C (1998) On the climatic implications of volcanic cooling. *J Geophys*  
422 *Res* 103:5929–5941.

- 423 12. Lindzen RS, Chou M-D, Hou AY (2001) Does the Earth have an adaptive infrared iris? *Bull*  
424 *Amer Met Soc* 82:417–432.
- 425 13. Lindzen RS, Hou AY, Farrell BF (1982) The role of convective model choice in calculating  
426 the climate impact of doubling CO<sub>2</sub>. *J Atmos Sci* 39:1189-1205.
- 427 14. Kanamitsu M, et al. (2002) NCEP/DOE AMIP-II Reanalysis (R-2). *Bull Amer Met Soc*  
428 83:1631–1643.
- 429 15. Barkstrom BR (1984) The Earth Radiation Budget Experiment (ERBE). *Bull Am Meteorol*  
430 *Soc* 65:1170–1185.
- 431 16. Wielicki BA, et al. (1998) Clouds and the Earth's Radiant Energy System (CERES):  
432 Algorithm overview. *IEEE Trans Geosci Remote Sens* 36:1127–1141.
- 433 17. Wong T, et al. (2006) Reexamination of the observed decadal variability of the earth  
434 radiation budget using altitude-corrected ERBE/ERBS nonscanner WFOV Data. *J Climate*,  
435 19:4028–4040.
- 436 18. Matthews G, et al. "Compensation for spectral darkening of short wave optics occurring on  
437 the Clouds and the Earth's Radiant Energy System," in *Earth Observing Systems X*, edited  
438 by James J. Butler, Proceedings of SPIE Vol. 5882 (SPIE, Bellingham, WA, 2005) Article  
439 588212.
- 440 19. Young DF, et al. (1998) Temporal Interpolation Methods for the Clouds and Earth's Radiant  
441 Energy System (CERES) Experiment. *J Appl Meteorol* 37:572–590.
- 442 20. Roe GH, Baker MB (2007) Why is climate sensitivity so unpredictable? *Science* 318:629.
- 443 21. Charney JG, et al. (1979), *Carbon Dioxide and Climate: A Scientific Assessment*, National  
444 Research Council, Ad Hoc Study Group on Carbon Dioxide and Climate. National Academy  
445 Press, Washington, DC, 22pp.

- 446 22. Forster PM, Taylor KE (2006) Climate forcing and climate sensitivities diagnosed from  
447 coupled climate model integrations. *J Climate* 19:6181–6194.
- 448 23. Murphy DM, et al. (2009) An observationally based energy balance for the Earth since 1950.  
449 *J Geophys Res* 114:D17107.
- 450 24. Newman M, Sardeshmukh PD, Penland C (2009) How important is air-sea coupling in  
451 ENSO and MJO Evolution? *J Climate* 22:2958–2977.
- 452 25. Lindzen RS (2007) Taking greenhouse warming seriously. *Energy & Environment* 18:937–  
453 950.
- 454 26. Douglass DH, Christy JR, Pearson BD, Singer SF (2007) A comparison of tropical  
455 temperature trends with model predictions. *Int J Climatol* 28:1693–1701.
- 456 27. Schwartz SE (2008) Reply to comments by G. Foster et al., R. Knutti et al., and N. Scafetta,  
457 on “Heat capacity, time constant, and sensitivity of Earth’s climate system”. *J Geophys Res*  
458 113:D15195.
- 459 28. Hansen J, et al. (1993) How sensitive is the world’s climate? *Natl Geogr Res Explor* 9:142–  
460 158.
- 461 29. Crowley TJ, North GR (1991) *Paleoclimatology*. Oxford Univ Press, NY, 339pp.
- 462 30. Lindzen RS (1993) Climate dynamics and global change. *Ann Rev Fl Mech* 26:353–378.

463 **Table Legends**

464 **Table 1.** Mean±standard error of the variables for the likely lag for the observations. The units  
465 for the slope are  $W m^{-2} K^{-1}$ . Also shown are the estimated mean and range of equilibrium  
466 climate sensitivity (in K) for a doubling of  $CO_2$  for 90%, 95%, and 99% confidence levels.

467 **Table 2.** Regression statistics between  $\Delta Flux$  and  $\Delta SST$  and the estimated feedback factors ( $f$ )  
468 for LW, SW, and total radiation in AMIP models; the slope is  $\Delta Flux/\Delta SST$ , N is the number of  
469 the points or intervals, R is the correlation coefficient, and SE is the standard error of  
470  $\Delta Flux/\Delta SST$ .

471 **Table 3.** Comparison of model equilibrium climate sensitivities (in K) for a doubling of  $CO_2$   
472 defined from IPCC AR4 and estimated from feedback factors in this study. The obvious  
473 difference between two columns labeled ‘sensitivity’ is discussed in more detail in the last  
474 paragraph of section 3.1. The estimated climate sensitivities for models as well as their  
475 confidence intervals are given for 90%, 95%, and 99% confidence levels.

476

477 **Figure Legends**

478 **Fig. 1.** A schematic for the behavior of the climate system in the absence of feedbacks (a), in the  
479 presence of feedbacks (b).

480 **Fig. 2.** Tropical mean (20°S to 20°N latitude) 36-day averaged and monthly sea surface  
481 temperature anomalies with the centered 3-point smoothing; the anomalies are referenced to the  
482 monthly means for the period of 1985 through 1989. Red and blue colors indicate the major  
483 temperature fluctuations exceeding 0.1°C used in this study. The cooling after 1998 El Niño is  
484 not included because of no flux data is available for this period (viz. Fig. 3).

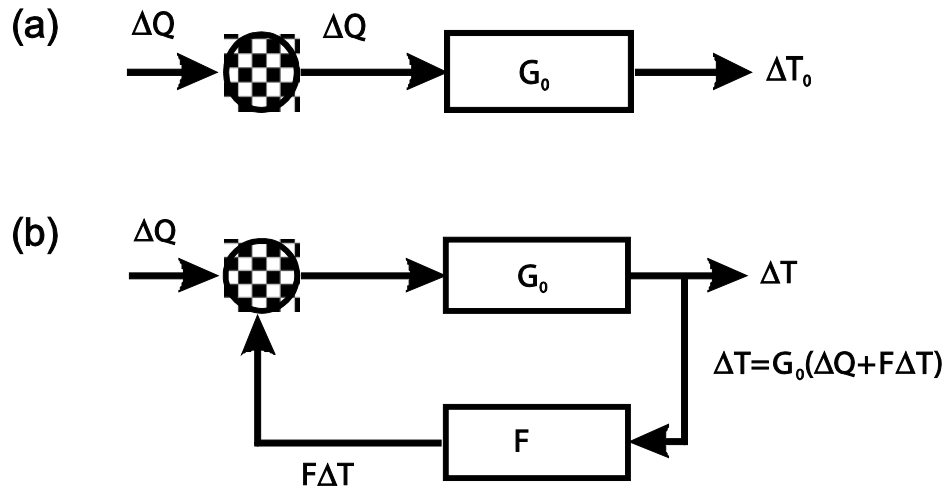
485 **Fig. 3.** The same as Fig. 2 but for outgoing longwave (red) and reflected shortwave (blue)  
486 radiation from ERBE and CERES satellite instruments. 36-day averages are used to compensate  
487 for the ERBE precession. The anomalies are referenced to the monthly means for the period of  
488 1985 through 1989 for ERBE, and 2000 through 2004 for CERES. Missing periods are the same  
489 as reported in ref. 17.

490 **Fig. 4.** The impact of smoothing and leads and lags on the determination of the slope (top) as  
491 well as on the correlation coefficient,  $R$ , of the linear regression (bottom).

492 **Fig. 5.** Sensitivity vs. feedback factor.

493 **Fig. 6.** Same as Fig. 4, but for the 10 CMIP models (black dots); GISS model was excluded  
494 because only few intervals of SST are obtained. The values for the 3-month smoothing in Fig. 4  
495 are superimposed by red dots.

496

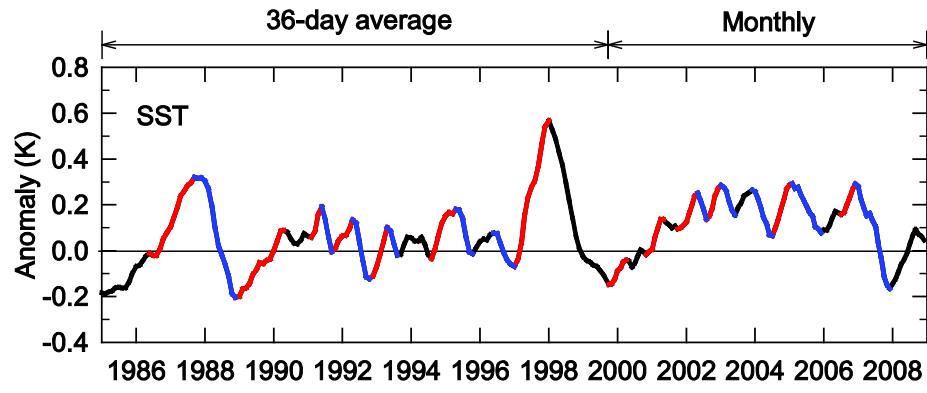


497

498 Figure 1

499

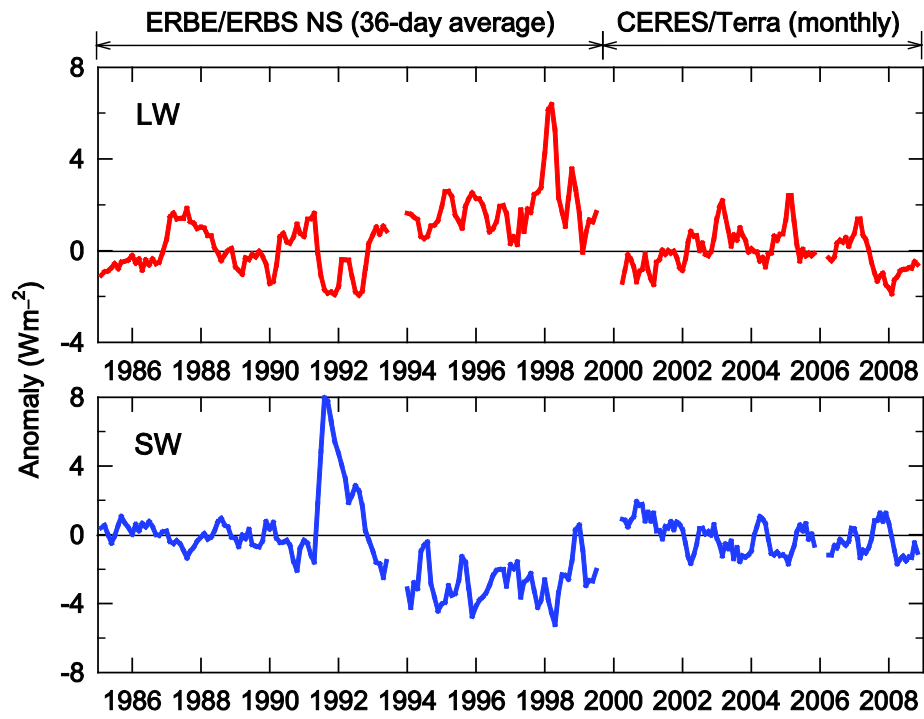




500

501 Figure 2

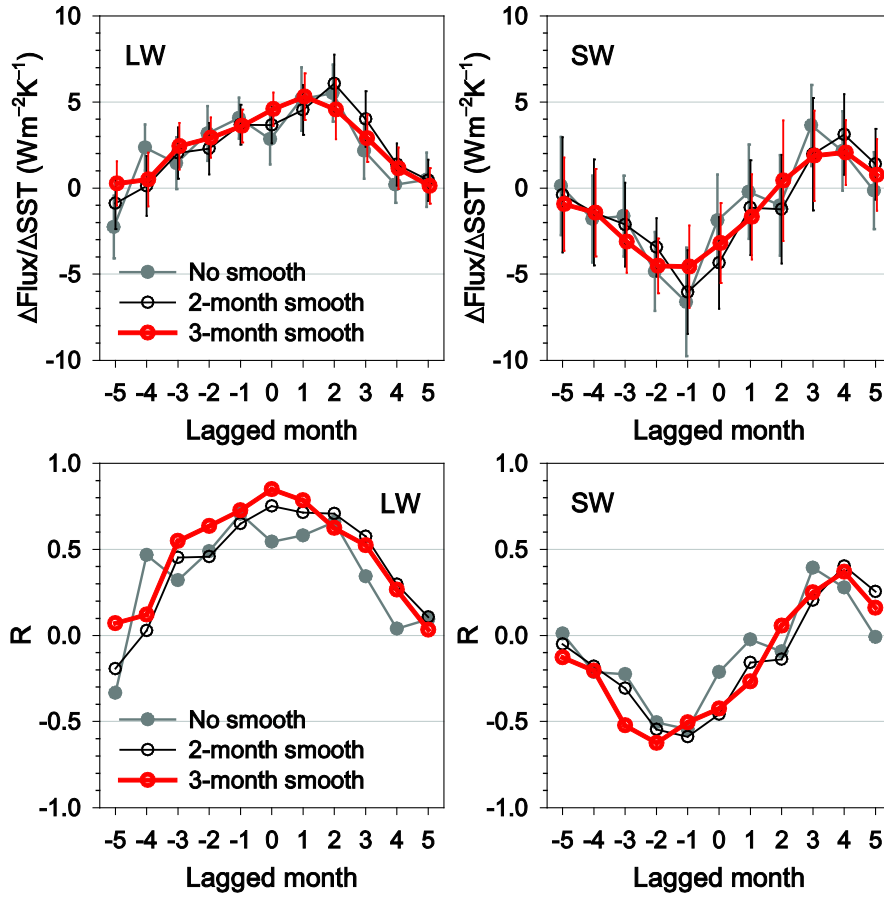
502



503

504 Figure 3

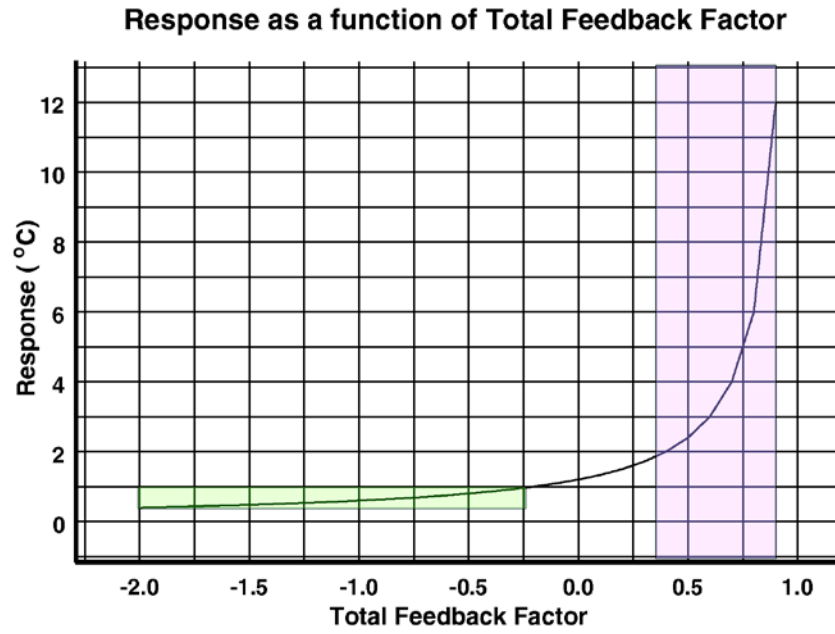
505



506

507 Figure 4

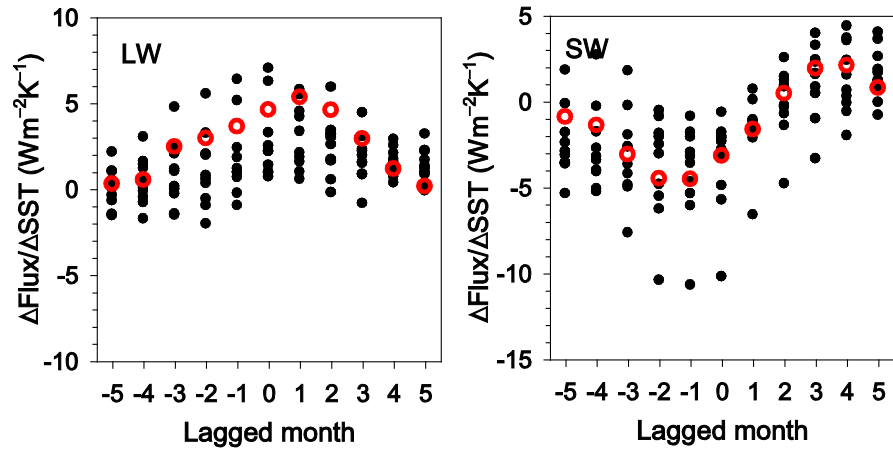
508



509

510 Figure 5

511



512

513 Figure 6

1 **Supporting Information**

2

3 **On the observational determination of climate sensitivity and its implications**

4

5 Richard S. Lindzen<sup>\*</sup>, and Yong-Sang Choi<sup>†</sup>

6

7 <sup>\*</sup>Program in Atmospheres, Oceans, and Climate, Massachusetts Institute of Technology,

8 Cambridge, MA 02142 USA

9 <sup>†</sup>Department of Environmental Science and Engineering, Ewha Womans University,

10 Seoul, 120-750 Korea

11

12 **1. Concentration of climate feedbacks in the tropics**

13 Although, in principle, climate feedbacks may arise from any latitude, there are substantive  
14 reasons for supposing that they are, indeed, concentrated mostly in the tropics. The most  
15 prominent model feedback is that due to water vapor, where it is commonly noted that models  
16 behave as though relative humidity were fixed. Pierrehumbert (31) examined outgoing radiation  
17 as a function of surface temperature theoretically for atmospheres with constant relative humidity.  
18 His results are shown in Fig. S1.

19 Relative humidity is low in the extratropics, while it is high in the extratropics. We see that for  
20 extratropical conditions, outgoing radiation closely approximates the Planck black body radiation  
21 (leading to small feedback). However, for tropical conditions, increases in outgoing radiation are  
22 suppressed, implying substantial positive feedback. There are also good reasons to suppose that  
23 cloud feedbacks are largely confined to the tropics. In the extratropics, clouds are mostly

24 stratiform clouds that are associated with ascending air while descending regions are cloud-free.  
25 Ascent and descent are largely determined by the large scale wave motions that dominate the  
26 meteorology of the extratropics, and for these waves, we expect approximately 50% cloud cover  
27 regardless of temperature. On the other hand, in the tropics, upper level clouds, at least, are  
28 mostly determined by detrainment from cumulonimbus towers, and cloud coverage is observed  
29 to depend significantly on temperature (32). As noted by LCH01, with feedbacks restricted to the  
30 tropics, their contribution to global sensitivity results from sharing the feedback fluxes with the  
31 extratropics. This leads to the factor of 2 in Eq. (6). The choice of larger factor leads to smaller  
32 contribution of tropical feedback to global sensitivity, but the effect on the climate sensitivity  
33 estimated from the observation is minor. For example, with the factor of 3, climate sensitivity  
34 from the observation and the models is 0.8 K and a higher value (between 1.3 K and 6.4 K),  
35 respectively. With the factor of 1.5, global equilibrium sensitivity from the observation and the  
36 models is 0.6 K and any value higher than 1.6 K, respectively. Note that, as in LCH01 (12), we  
37 are not discounting the possibility of feedbacks in the extratropics, but rather we are focusing on  
38 the tropical contribution to global feedbacks.

39

## 40 **2. Origin of Feedbacks**

41 While the present analysis is a direct test of feedback factors, it does not provide much insight  
42 into detailed mechanism. Nevertheless, separating the contributions to  $f$  from long wave and  
43 short wave fluxes provides some interesting insights. The results are shown in Tables 1 and 2. It  
44 should be noted that the consideration of the zero-feedback response, and the tropical feedback  
45 factor to be half of the global feedback factor is actually necessary for our measurements from  
46 the Tropics; however, these were not considered in Lindzen and Choi (4). Accordingly, with

47 respect to separating longwave and shortwave feedbacks, the interpretation by Lindzen and Choi  
48 (4) needs to be corrected. These tables show recalculated feedback factors in the presence of the  
49 zero-feedback Planck response. The negative feedback from observations is from both longwave  
50 and shortwave radiation, while the positive feedback from models is usually but not always from  
51 longwave feedback.

52 As concerns the infrared, there is, indeed, evidence for a positive water vapor feedback (33),  
53 but, if this is true, this feedback is presumably cancelled by a negative infrared feedback such as  
54 that proposed by LCH01 on the iris effect. In the models, on the contrary, the long wave  
55 feedback appear to be positive (except for two models), but it is not as great as expected for the  
56 water vapor feedback (10, 33). This is possible because the so-called lapse rate feedback as well  
57 as negative longwave cloud feedback serves to cancel the TOA OLR feedback in current models.  
58 Table 2 implies that TOA longwave and shortwave contributions are coupled in models (the  
59 correlation coefficient between  $f_{LW}$  and  $f_{SW}$  from models is about  $-0.5$ ). This coupling most  
60 likely is associated with the primary clouds in models — optically thick high-top clouds (34). In  
61 most climate models, the feedbacks from these clouds are simulated to be negative in longwave  
62 and strongly positive in shortwave, and dominate the entire cloud feedback (34). Therefore, the  
63 cloud feedbacks may also serve to contribute to the negative OLR feedback and the positive  
64 SWR feedback. New spaceborne data from the CALIPSO lidar (CALIOP; 35) and the CloudSat  
65 radar (CPR; 36) should provide a breakdown of cloud behavior with altitude which may give  
66 some insight into what exactly is contributing to the radiation.

67

### 68 **3. Simple model analysis**

69 The model system was basically forced by random internal non-radiative forcing changing



70 SST. Integration is done at monthly time steps. Fig. S2 compares the simple regression method  
71 and our method; given the feedback function  $F = 6 \text{ W m}^{-2} \text{ K}^{-1}$  (it indicates negative feedback as  
72 it is larger than Planck response  $3.3 \text{ W m}^{-2} \text{ K}^{-1}$ ), the system was additionally forced by random  
73 internal radiative forcing (the root mean square (RMS) is set to be 10% of RMS of internal non-  
74 radiative forcing, considering the observed magnitude of cloud forcing over the tropics), and  
75 transient external radiative forcing ( $0.4 \text{ W m}^{-2}$  per decades by increasing  $\text{CO}_2$ ) (3). The  
76 maximum R occurs at small (zero or a month) lag and the corresponding  $\Delta\text{Flux}/\Delta T$  ( $5.7 \text{ W m}^{-2}$   
77  $\text{K}^{-1}$ ) is close to the assumed  $F$ , whereas the simple regression method underestimates  $\Delta\text{Flux}/\Delta T$   
78 ( $3.2 \text{ W m}^{-2} \text{ K}^{-1}$ ); the difference is statistically significant by a Monte-Carlo test (with 100  
79 repetitions).

80 We now attempt to confine the simulation to SW radiation. This requires separation of a  
81 feedback function  $F$  to those for SW and LW radiation (i.e.,  $F = F_{\text{SW}} + F_{\text{LW}}$ ). For convenience,  
82  $F_{\text{LW}}$  is set to zero. In SW, a positive feedback function indicates negative feedback. In addition,  
83 the transient external forcing originates from LW radiation and can be removed for the  
84 simulation of SW radiation. Sensitivity to the feedback function  $F$  for SW radiation is shown in  
85 Fig. S3. A smaller feedback function turns out to have maximum R at larger lag, and the  
86 estimated climate feedbacks are the lagged response though it is somewhat less reliable than  
87 those at zero lag; the uncertainty of the feedback estimate from the lagged response is within  
88  $\pm 0.3$  for a small feedback function between  $-2$  and  $2$ . However, it is also clearly found that the  
89 smoother with a time window longer than three months effectively reduces the uncertainty and  
90 gives a much more accurate estimate of feedback. This indicates the necessity of stronger  
91 smoothing to minimize SST variations that are primarily forced by non-feedback atmospheric  
92 changes, but to retain SST variations that are primarily forcing atmospheric changes.

93 While the present SW simulation is for the absence of  $F_{LW}$ , many climate models as well as  
94 nature appear to have a positive  $F_{LW}$ , as shown by the slopes for LW in Tables 1 and 2. With a  
95 positive  $F_{LW}$ , the system with  $F_{SW} < -2$  does not have to be very unstable and can also generate  
96 the sinusoidal shape of the slopes with respect to lags. In any of the cases, with either no internal  
97 cloud-induced radiative change or the prescribed temperature variation,  $\Delta\text{Flux}/\Delta T$  at zero lag  
98 (with maximum R) is always identical to the assumed  $F$ . This explains why AMIP systematically  
99 shows maximum R at zero lag, while CMIP does not.

100

101 **References**

- 102 31. Pierrehumbert RT (2009) Principles of planetary climate. Cambridge University Press, 688pp.
- 103 32. Rondanelli R, Lindzen RS (2008) Observed variations in convective precipitation fraction  
104 and stratiform area with sea surface temperature. *J Geophys Res* 113:D16119.
- 105 33. Soden BJ, Jackson DL, Ramaswamy V, Schwarzkopf MD, Huang X (2005) The radiative  
106 signature of upper tropospheric moistening. *Science* 310:841–844.
- 107 34. Webb MJ, et al. (2006) On the contribution of local feedback mechanisms to the range of  
108 climate sensitivity in two GCM ensembles. *Clim Dyn* 27:17–38.
- 109 35. Winker DM, Hunt WH, McGill MJ (2007) Initial performance assessment of CALIOP.  
110 *Geophys Res Lett* 34:L19803.
- 111 36. Im E, Durden SL, Wu C (2005) Cloud profiling radar for the Cloudsat mission. *IEEE Trans*  
112 *Aerosp Electron Syst* 20:15–18.

113

114 **Figure Legends**

115 **Fig. S1.** OLR vs. surface temperature for water vapor in air, with relative humidity held fixed.

116 The surface air pressure is 1bar. The temperature profile is the water/air moist adiabat.

117 Calculations were carried out with the Community Climate Model radiation code (31).

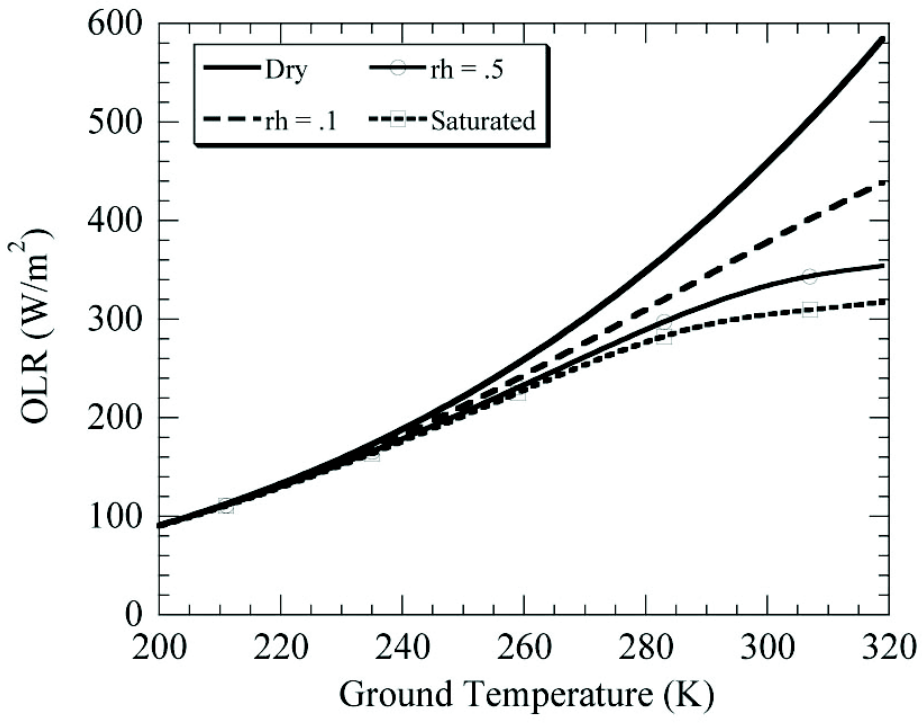
118 **Fig. S2.** Comparison between simple regression method and the method used in this study, based  
119 on simple model results.

120 **Fig. S3.** Sensitivity of the method used in this study to feedback functions, based on simple  
121 model results.

122 **Fig. S4** Comparison of outgoing longwave radiation from AMIP models (black) and the  
123 observations (red) shown in Fig. 3.

124 **Fig. S5** Comparison of reflected shortwave radiation from AMIP models (black) and the  
125 observations (blue) shown in Fig. 3.

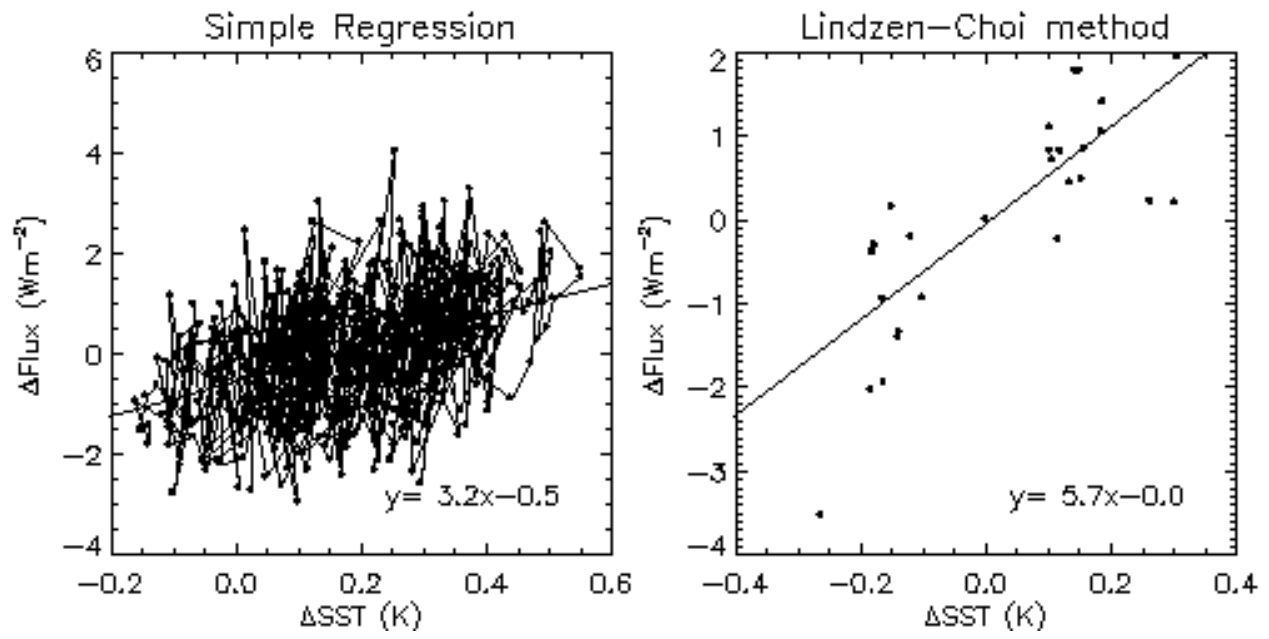
126



127

128 Figure S1

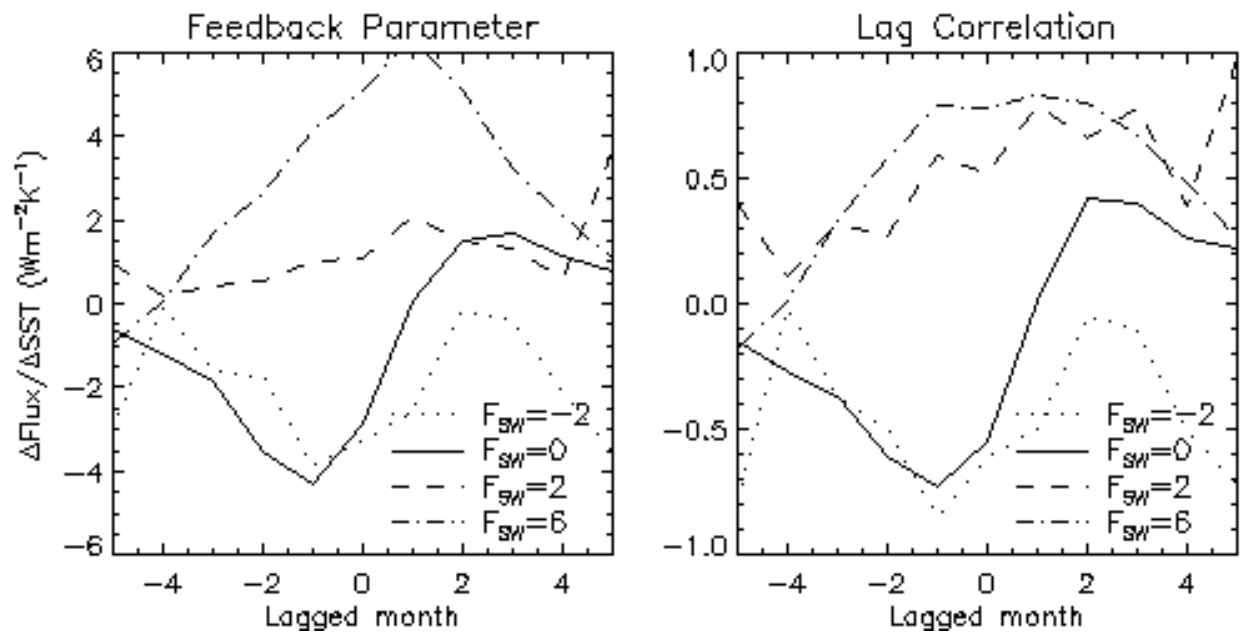
129



130

131 Figure S2

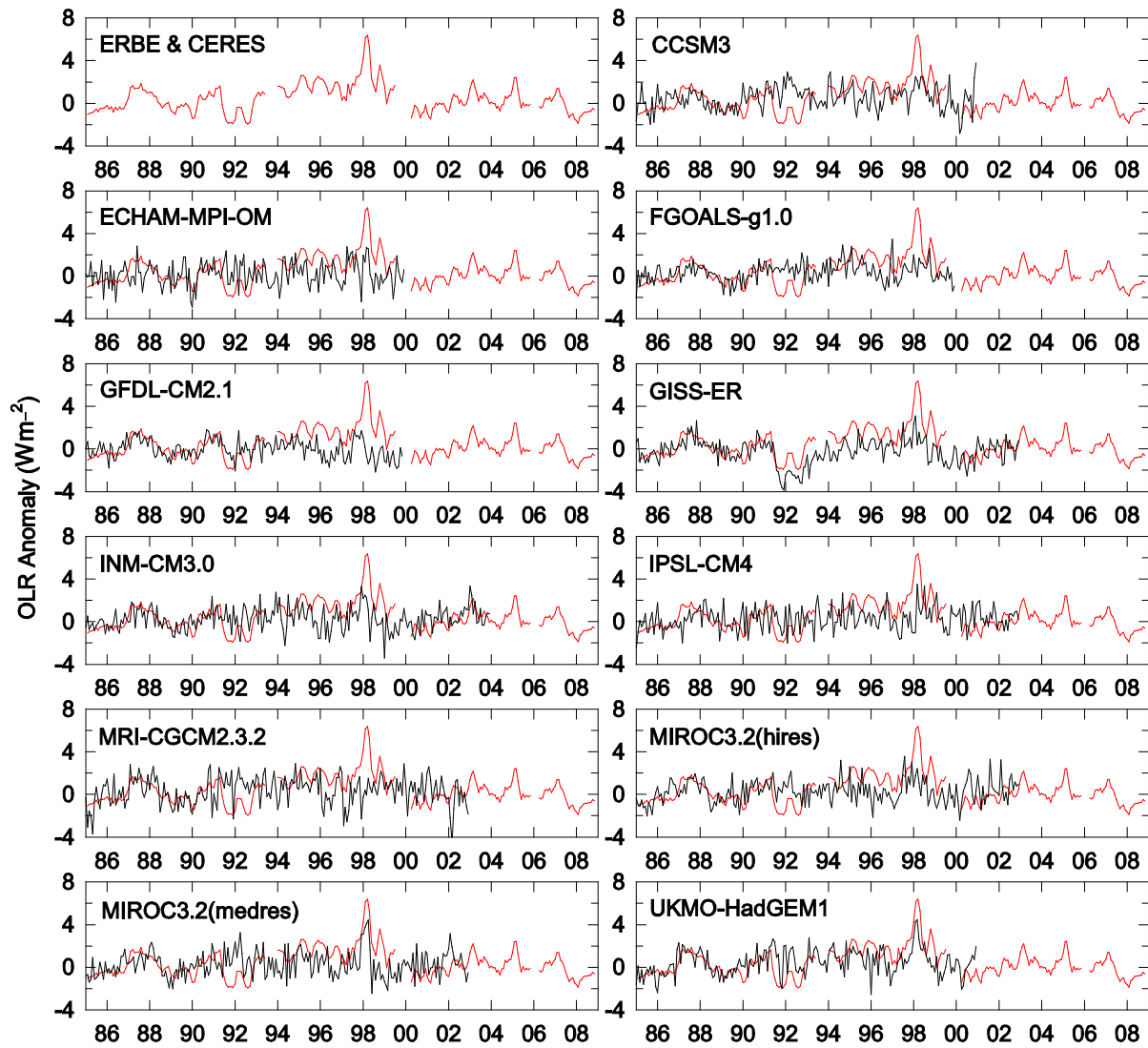
132



133

134 Figure S3

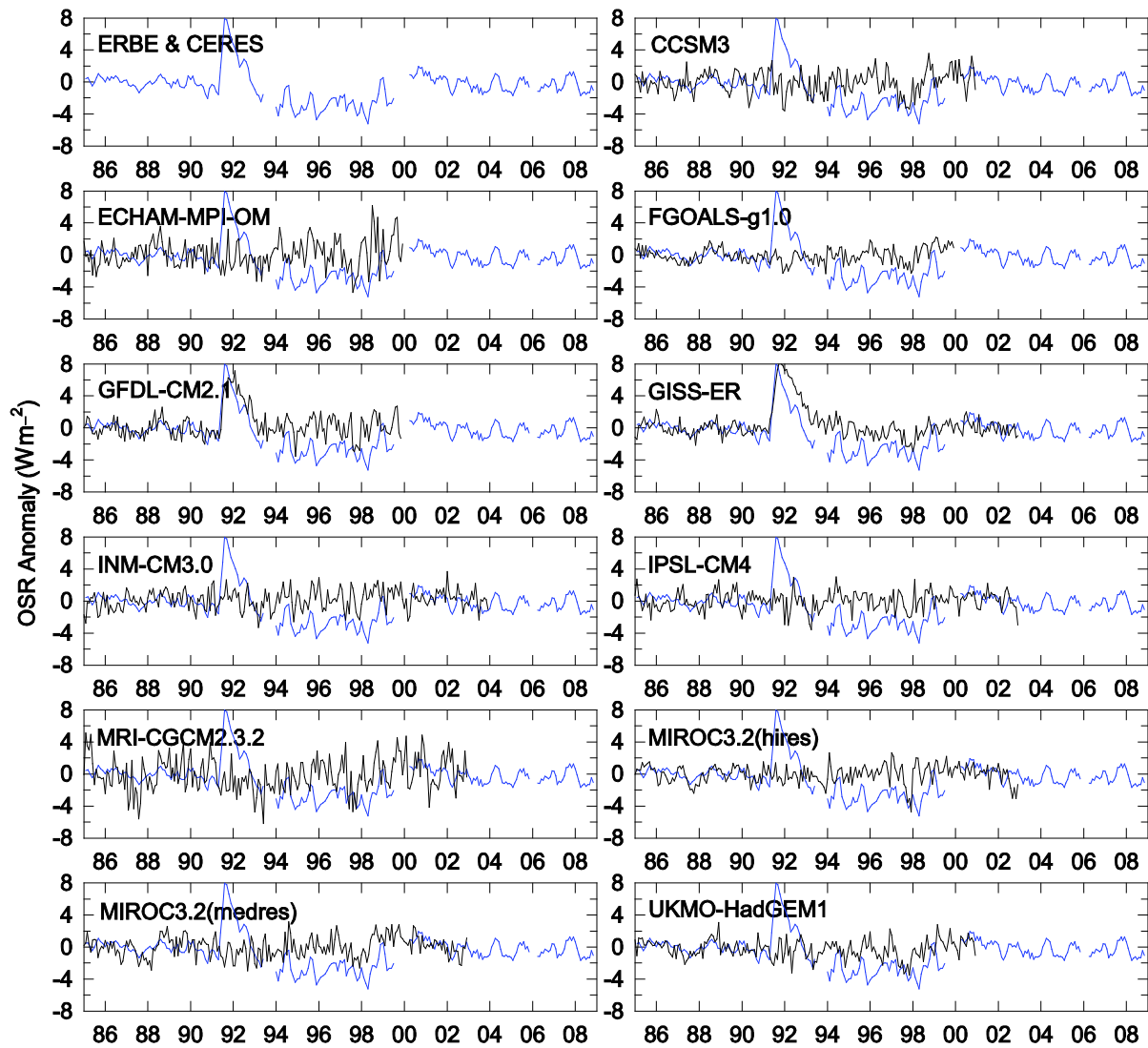
135



136

137 Figure S4





138

139 Figure S5

140